Zhu, Z., Ren, H., Incecik, A., Lin, T., Li, C., & Zhou, X. (2024). A novel method for determining the neutral axis position of the asymmetric cross section and its application in the simplified progressive collapse method for damaged ships. Ocean Engineering, 301, Article 117390. https://doi.org/10.1016/j.oceaneng.2024.117390

A Novel Method for Determining the Neutral Axis Position of the Asymmetric Cross Section and its Application in the Simplified Progressive Collapse Method for Damaged Ships

Zhiyao Zhu[a,b], Huilong Ren[a,b], Atilla Incecik[c], Tong Lin[c], Chenfeng Li[a,b], Xueqian Zhou[a,b,*]

[a] *College of Shipbuilding Engineering, Harbin Engineering University, Harbin, 150001, China*
[b] *International Joint Laboratory of Naval Architecture and Offshore Technology between Harbin Engineering University and Lisbon University, Harbin, 150001, China*
[c] *Department of Naval Architecture, Ocean and Marine Engineering, University of Strathclyde, 100 Montrose Street, Glasgow, G4 0LZ, UK*
[d] *Marine Design & Research Institute of China, Shanghai, 200011, China*
[*] Corresponding author: xueqian.zhou@hrbeu.edu.cn (X. Zhou)

ABSTRACT: Ultimate strength is an important factor of the safety of intact or damaged ship structures. The simplified progressive collapse method is a commonly used iterative method for obtaining the accurate ultimate strength of ships. Since the accuracy of the neutral axis position directly affects the accuracy of the ultimate strength, the force equilibrium criterion and the force vector equilibrium criterion are adopted to search for the height and angle of the neutral axis, especially for damaged ships. However, the search for the neutral axis position based on the two criteria requires iterative computation, and it decreases the calculation efficiency. In this paper, the relationship between the criterion results and the neutral axis position is studied, and it is found that the relationship is approximately linear. Then a new iterative method based on the linear equation is proposed to obtain the neutral axis position and it is adopted to improve the simplified progressive collapse method. Finally, the new method is used to calculate the damaged VLCC. The comparison of the ultimate strength results shows that the improved simplified progressive collapse method based on the linear equation has satisfying efficiency and accuracy.
KEYWORDS: ultimate strength; neutral axis; force equilibrium criterion; force vector equilibrium criterion; linear equation

Acronyms

NFEM	Nonlinear Finite Element Method
FEC	Force Equilibrium Criterion
FVEC	Force Vector Equilibrium Criterion
IFVEC	Improved Force Vector Equilibrium Criterion
NA	Neutral Axis—the one meeting the criteria
CNA	Computation Neutral Axis—the trial neutral axis used for computation

Nomenclature

M	bending moment
χ	curvature
M_U	ultimate strength
δ_1	specified tolerance on zero value in the HCSR
F_{ic}	compressive force of unit *i*

F_{it} tensile force of unit *i*

δ_2 specified tolerance for the FEC

$\vec{F}$ sum of force vectors for all units

$\vec{M}$ sum of force moment vectors for all units

δ_3 specified tolerance on zero value for the FVEC

C_c centroid of the compressive force area

C_t centroid of the tensile force area

y_c *y*-coordinate of C_c

y_t *y*-coordinate of C_t

δ_3' specified tolerance on zero value for the IFVEC

y_i *y*-coordinate of unit *i*

z_i *z*-coordinate of unit *i*

a_i cross-sectional area of unit *i*

l length of the unit

z_j height of the NA

θ_j angle of the NA

h_{ij} distance between element *i* and the NA at the curvature χ_j

h_{ij}' distance between element *i* and the CNA at the curvature χ_j

Δz_{ij} vertical distance between the NA and the CNA at the curvature

$\mathrm{V}h_{ij}$ distance between the NA and the CNA at the curvature χ_j

Δl_{ij} length increment of the NA at the curvature χ_j

$\Delta l_{ij}'$ length increment of the CNA at the curvature χ_j

ε_{ij} strain of unit *i* due to the NA at the curvature χ_j

ε_{ij}' strain of unit *i* due to the CNA at the curvature χ_j

$\Delta\varepsilon_{ij}$ strain difference between ε_{ij} and ε_{ij}' at the curvature χ_j

$\Delta\sigma_{ij}$ stress increment of unit *i* at the curvature χ_j

E_{Tij} tangent modulus of unit *i* at the curvature χ_j

F_{ij} force of unit *i* due to the NA at the curvature χ_j

F_{ij}' force of unit *i* due to the CNA at the curvature χ_j

ΔF_{ij} force increment of unit *i* at the curvature

k_{ij} slope of the force increment of unit *i* at the curvature

$\Delta\theta$ angle increment of the CNA

ΔP_1 FEC result due to the translation of the CNA

k_{P1} ratio of the result ΔP_1 of the FEC to the distance Δz

ΔP_2 FEC result due to the rotation of the CNA

k_{P2} ratio of the result ΔP_2 of the FEC to the angle $\Delta\theta$

Δs_1 result for the IFVEC due to the translation of the CNA

k_{s1} ratio of the result Δs_1 of the IFVEC to the distance Δz

Δs_2 result for the IFVEC due to the rotation of the CNA

k_{s2} ratio of the result Δs_2 of the IFVEC to the angle $\Delta\theta$

1. Introduction

Ships sailing at sea may be damaged due to collision, grounding, fire or other accidents. These accidents may lead to cargo damage, environmental pollution, ship sinking and even loss of lives. According to the report provided by the EMSA (2019), there were 3174 casualties or accidents in 2018, of which 95 were very serious and 25 ships were lost. In the event of accidents involving damage to the hull structures, the structural safety does not only concern of thie ship itself, but is also vital to the safety of cargo and the personnel onboard. Depending on whether there is flooding, the ship may be still foating upright or heeling. The former is a problem of asymmetric structure and the latter is of asymmetric structure and hydrostatic/hydrodynamic load. For instance, Ro-Ro vessel Modern Express lost the stability and heeled at 51° in heavy weather (Chan et al., 2001), and the load condition is more complicated than intact hull. It was reported that the horizontal load of the damaged ship is 1.73 times larger than the vertical load (Chan et al., 2003). For the safety of ships, it is necessary to study the structural behavior of damage ships and establish proper methods for the assessment of structures

Many researchers have investigated the safety of the damaged ship structures (Tekgoz et al, 2018 ; Hussein and Guedes Soares, 2009; Fang and Das, 2005; Shi and Gao, 2021; Fujikubo et al, 2012; Luís, 2007), and it is found that the key to the assessment is the accuracy of the ultimate strength, and the standard computation method is the Nonlinear Finite Element Method (NFEM) (Kuznecovs et al, 2020; Faisal et al, 2017; Liu and Amdahl, 2012; Hu et al, 2018; Parunov et al, 2018) and the Simplified Progressive Collapse Method (Smith method) (Campanile et al, 2015; Ahn et al, 2011; Campanile et al, 2014). The NFEM accounts for the initial imperfection, the material nonlinearity and geometric nonlinearity, and the influence of the adjacent parts, which can produce accurate results. However, the method requires much time for modeling and computation. The simplified progressive collapse method proposed by Smith (1977), i.e. the so-called Smith method, discretizes the cross-section of ship hull into stiffened plate units, plate units, and hard corner units. Strain increases with increasing curvature, and then the stress of each unit is obtained by the stress-strain curves. According to the Force Equilibrium Criterion (FEC) (Choung et al, 2012; Choung et al, 2014), the Neutral Axis (NA) location of the cross-section is obtained. Then the bending moments of the units and the bending moment of the cross-section are obtained. Finally, the bending moment-curvature relationship curve is obtained and the peak is the ultimate strength. Because the computational time of the Smith method is much less and the accuracy is aslo satisfying, it has been widely adopted for preliminary designs and researches (IACS, 2014; LR, 2020).

The strain-stress relationship and the location of the NA play key roles in ensuring the computational accuracy of the Smith method. The rules such as HCSR (IACS, 2014) proposed a variety of strain-stress relationship curves and the FEC to search the location of the NA to obtain the accurate ultimate strength, but the method is only applicable to symmetrical ships because the rotation of the NA is not considered. For damage ships, the NA not only translates but also rotates with the increase of the curvature, and neglecting the rotation will lead to inaccurate estimates. To overcome this drawback, Choung et al (2012; 2014) proposed a Force Vector Equilibrium Criterion (FVEC) to obtain the rotation of NA. According to the two criteria, Li et al. (2017) proposed the linear search method to obtain the location of NA. Referring to the location of NA for the previous curvature, the NA is translated and the results of the FEC are calculated at

different height, and the minimal result for the height is the required height. Then the NA is rotated, and the minimal result of the FVEC for the angle is the required angle. Because the method cannot track the translation and the rotation of NA at the same time, Li et al (2018) adopted the Particle Swarm Optimization (PSO) algorithm for searching the location of NA. The method takes the translation and rotation as the two attributes of the particles and searches for the global optimum result of the two criteria for obtaining the location of NA. The accuracy of the PSO based method is good, but the computation efficiency is limited, which offsets the advantage of the Smith Method.

In this study, aiming at efficicent and accurate estimation based on the Smith method, the results are obtained using the FEC and FEVC for a systematic set of locations of NA, investigation of the results and the locations shows that there is a linear relationship between them. Based on this finding, and an improved Smith method for determinating the NA is proposed. The accuracy and efficencity of the method are validated for the ultimate strength of a VLCC, and the tolerances for the FEC and FVEC are also discussed.

2. Simplified Progressive Collapse Method

2.1 Calculation process of the traditional simplified progressive collapse method

The calculation process of the Smith method is straightfoward. The cross-section of the hull structure is divided into different types of units. As the curvature increases, the strain and stress in the units are obtained at each step. The location of NA is obtained according to the FEC, then the unit moments are calculated and the sum is the cross-section moment at each step. Finally, the bending moment-curvature curve is obtained, and the peak of the curve is the ultimate strength.

To assess the ultimate strength of the ship, the calculation process of the Smith method is shown as follows:

(1) Divide the cross-section of the ship into stiffener plate units, plate units, and hard corner units;

(2) Define the stress-strain relationships for all types of units;

(3) Initialize the curvature and the NA for the first incremental step;

(4) Calculate the stress and the strain of each unit;

(5) Obtain the location of NA at each curvature according to the FEC;

(6) Calculate the moment by summing the contributions of all units;

(7) Compare the moment in the current incremental step with the previous moment. If the slope in the M-χ relationship is less than a negative fixed value, terminate the process and define the peak value of M_U. Otherwise, increase the curvature by the amount of χ_F and go to Step 4.

The calculation process is shown in Fig. 1.

The accuracy of the Smith method depends on the following factors:

(1) The accuracy of the stress-strain relationships of units;

(2) The accuracy of the location of NA at different curvatures.

The stress-strain relationships of the units provided by the HCSR have been widely used by many researchers and engineers. The location of NA is obtained according to the FEC as follows (Smith, 1977):

$$\left|\frac{\sum F_{ic}-\sum F_{it}}{\sum F_{ic}+\sum F_{it\,t}}\right|<\delta_2 \tag{1}$$

where F_c is the sum of the compressive forces of all units, and F_t the sum of the tensile forces of all units, and δ_2 the specified tolerance of zero value for the FEC and which usually takes the value of 0.01.

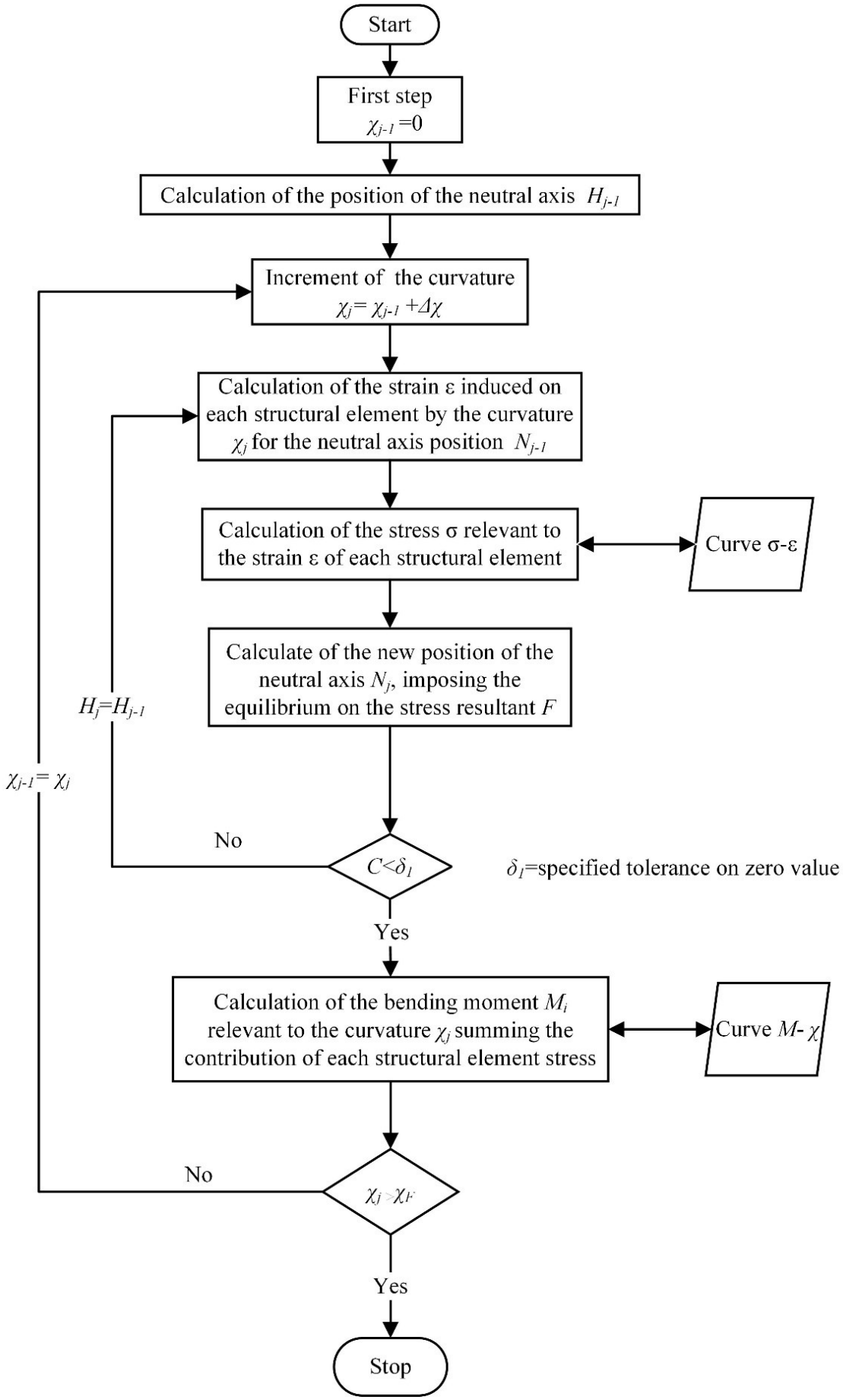

Fig. 1. The calculation process of the Smith method (IACS, 2014).

2.2 *Imporved criterion for the symmetric cross-section*

The FEC is only used to obtain the height of NA. However, when the cross-section of the ship is asymmetric, or the load is asymmetric, the NA will translate and rotate as the curvature increases. Therefore, application of the FEC alone will lead to incorrect estimates.

To obtain the angle of NA, the criterion of the FVEC was proposed (Choung et al, 2012; Choung, 2014):

$$\left|\cos^{-1}\left(\frac{\vec{F}\cdot\vec{M}}{|\vec{F}||\vec{M}|}\right)-\frac{\pi}{2}\right|<\delta_3 \tag{2}$$

where $\vec{F}$ is the sum of force vectors for all units, $\vec{M}$ the sum of force moment vectors for all units, δ_3 the specified tolerance on zero value for the FVEC and for which values less than 0.1° are recommended.

3. New method for obtaining the NA

3.1 Improved force vector equilibrium criterion for the symmetric cross-section

The force and the moment which satisfy the FVEC acting on the asymmetric cross-section are shown in Fig. 2. C_c is the centroid of the compressive force area, C_t is the centroid of the tensile force area, and the direction of the connecting line is defined as the direction of $\vec{F}$.

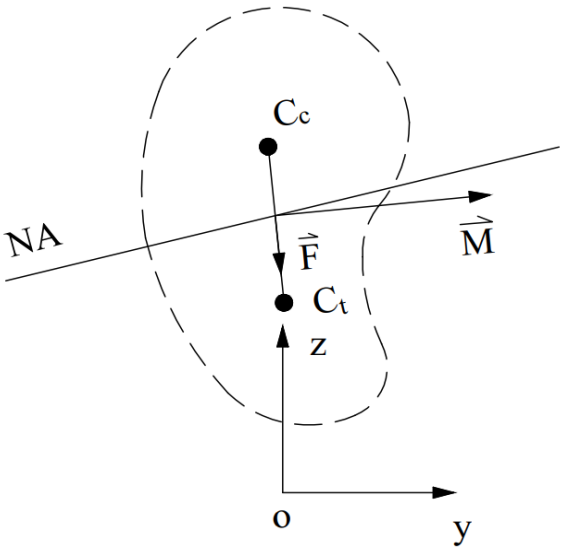

Fig. 2. Force and moment satisfying the FVEC acting on the asymmetric cross-section.

$\vec{F}$ is perpendicular to $\vec{M}$. If the direction of $\vec{M}$ is forced to be horizontal, the cross-section of Fig. 2 rotates, as shown in Fig. 3.

It is found that the *y*-coordinates of C_c and C_t are the same when $\vec{F}$ is vertical, then the Force Vector Equilibrium Criterion (IFVEC) is improved as follows:

$$|y_c - y_t| < \delta_3' \tag{3}$$

where y_c is the *y*-coordinate of C_c, and y_t the *y*-coordinate of C_t, and δ_3' the specified tolerance on zero value for the IFVEC.

The researches of Li et al. (2017) and Li et al (2018) showed that the results of the FEC and the FVEC are related to the height and angle of NA. Therefore, it is necessary to investigate the relationship between the results and the location. To simplify the study, the relationships are

investigated separately at first and then the influence between them is analyzed. The unit force is studied first, then the equilibrium criteria.

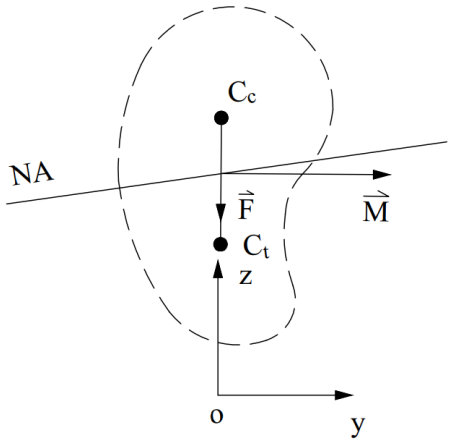

Fig. 3. Force and moment of the rotated cross-section.

3.2 Relationship between the CNA and unit force

To study the characteristics of NA, the cross-section is divided into independent units. For unit *i*, the coordinates are (y_i, z_i), and the cross-sectional area is a_i, and the length is l. If the curvature is χ_j, the height of NA that satisfies the two criteria simultaneously is z_j, the angle is θ_j, and the distance between unit *i* and the NA is h_{ij}, as shown in Fig.4. Because the NA is difficult to be obtained directly, the better method is assuming a new NA named the Computation Neutral Axis (CNA) for the solution process. The distance between unit *i* and the CNA is h'_{ij}. If the CNA does not satisfy the criteria, it is moved until the NA is found.

In the investigation of the relationship between the translation of NA and the force of the units, the NA and the CNA are parallel as no rotation is involved. The vertical distance between them is Δz_{ij}, and the relationship is shown in Fig. 4.

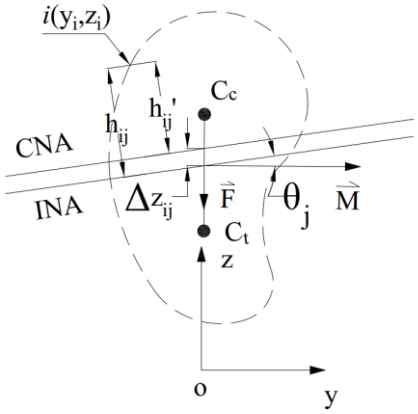

Fig. 4. Relationship between the NA and the CNA.

The distance Vh_{ij} between the NA and the CNA is:

$$Vh_{ij} = \left| h_{ij} - h'_{ij} \right| \tag{4}$$

The vertical distance Δz_{ij} between the two axes is:

$$Vz_{ij} = Vh_{ij} / \cos\theta_j \tag{5}$$

When the curvature is χ_j, the length increments Δl_{ij} of NA and $\Delta l'_{ij}$ of the CNA are calculated by:

$$\Delta l_{ij} = \chi_j h_{ij} \tag{6}$$

$$\Delta l'_{ij} = \chi_j h'_{ij} \tag{7}$$

The strains ε_{ij} and ε'_{ij} are obtained by:

$$\varepsilon_{ij} = \frac{\Delta l_{ij}}{l} = \frac{\chi_j h_{ij}}{l} \tag{8}$$

$$\varepsilon'_{ij} = \frac{\Delta l'_{ij}}{l} = \frac{\chi_j h'_{ij}}{l} \tag{9}$$

The strain difference $\Delta\varepsilon_{ij}$ between ε_{ij} and ε'_{ij} is:

$$\Delta\varepsilon_{ij} = \varepsilon'_{ij} - \varepsilon_{ij} = \frac{\chi_j (h'_{ij} - h_{ij})}{l} = \frac{\chi_j \Delta h_{ij}}{l} = \frac{\chi_j \Delta z_{ij} \cos\theta_j}{l} \tag{10}$$

The strain $\Delta\varepsilon_{ij}$ is small if the movement Δz_{ij} of the CNA is small, and stress $\Delta\sigma$ corresponding to strain $\Delta\varepsilon$ is also small, as shown in Fig. 5.

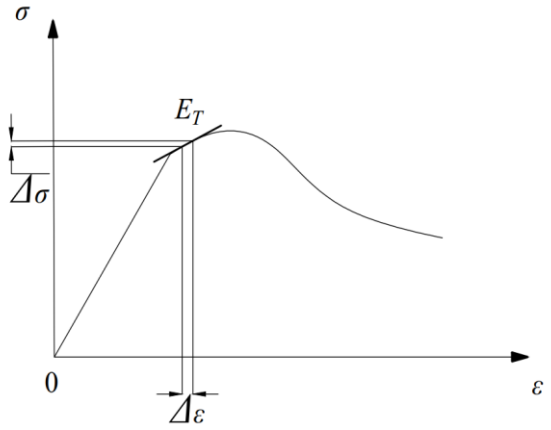

Fig. 5. Strain-stress curve of the unit.

It can be found that the relationship between $\Delta\varepsilon$ and $\Delta\sigma$ is nearly linear. Then the stress $\Delta\sigma_{ij}$ can be obtained:

$$\Delta\sigma_{ij} \approx E_{Tij}\Delta\varepsilon_{ij} \approx \frac{E_{Tij}\chi_j \Delta z_{ij}}{l} \tag{11}$$

If the stress of unit *i* corresponding to the NA and the CNA is σ_{ij} and σ'_{ij}, and the forces F_{ij} and F'_{ij} are calculated by:

$$F_{ij} = \sigma_{ij} a_i \tag{12}$$

$$F'_{ij} = \sigma'_{ij} a_i \tag{13}$$

The stress ΔF_{ij} can be obtained by:

$$\Delta F_{ij} = F'_{ij} - F_{ij} = \sigma'_{ij} a_i - \sigma_{ij} a_i = \Delta\sigma_{ij} a_i = \frac{E_{Tij}\chi_j \Delta h_{ij} a_i}{l} \tag{14}$$

Then,

$$F'_{ij} = \sigma_{ij} a_i + \frac{E_{Tij}\chi_j \Delta z_i a_i \cos\theta_j}{l} = \sigma_{ij} a_i + k_{ij}\Delta z_i a_i \tag{15}$$

where

$$k_{ij} = \frac{E_{Tij}\chi_j \cos\theta_j}{l} \tag{16}$$

where E_{Tij} is the tangent modulus of unit *i*.

To invetigate the relationship between the rotation of NA and the force of the units, the CNA is rotated about the NA, as shown in Fig. 6.

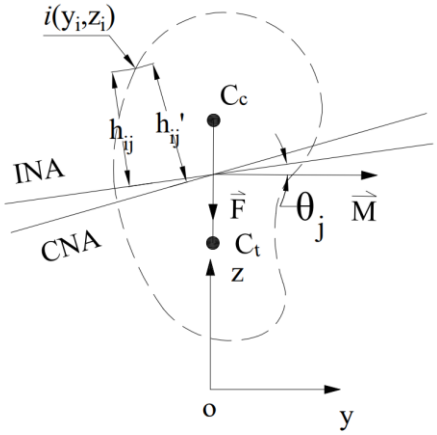

Fig. 6. Relationship between the CNA and the NA.

The distances between unit *i* and the two axes are:

$$h_{ij} = (z_i - z_j)\cos\theta_j + (y_i - y_j)\sin\theta_j \tag{17}$$

$$h'_{ij} = (z_i - z_j)\cos(\theta_j - \Delta\theta) + (y_i - y_j)\sin(\theta_j - \Delta\theta) \tag{18}$$

The distance between the two axes is:

$$\begin{aligned}\Delta h_{ij} &= (z_i - z_j)\cos(\theta_j - \Delta\theta) + (y_i - y_j)\sin(\theta_j - \Delta\theta) - (z_i - z_j)\cos\theta_j - (y_i - y_j)\sin\theta_j \\ &= (z_i - z_j)(\cos\theta_j \cos\Delta\theta_j + \sin\theta_j \sin\Delta\theta_j) + y_i(\sin\theta_j \cos\Delta\theta_j + \cos\theta_j \sin\Delta\theta_j) \\ &\quad -(z_i - z_j)\cos\theta_j - (y_i - y_j)\sin\theta_j\end{aligned} \tag{19}$$

If $\Delta\theta_j \to 0$, then,

$$\begin{aligned}\Delta h_{ij} &\approx (z_i - z_j)(\cos\theta_j + \Delta\theta\sin\theta_j) + (y_i - y_j)(\sin\theta_j + \Delta\theta\cos\theta_j) \\ &\quad -(z_i - z_j)\cos\theta_j - (y_i - y_j)\sin\theta_j \\ &\approx -\Delta\theta[(z_i - z_j)\sin\theta_j + (y_i - y_j)\cos\theta_j]\end{aligned} \tag{20}$$

Therefore,

$$F'_{ij} = \sigma_{ij}a_i + \frac{-\Delta\theta_j[(z_i - z_j)\sin\theta_j + (y_i - y_j)\cos\theta_j]E_{Tij}\chi_j a_i}{l} = \sigma_{ij}a_i + k_{ij}\Delta\theta_j a_i \tag{21}$$

and

$$k_{ij} = \frac{-[(z_i - z_j)\sin\theta_j + (y_i - y_j)\cos\theta_j]E_{Tij}\chi_j}{l} \tag{22}$$

3.3 Relationship between the CNA and the equilibrium criteria

(1) Relationship between the results for the FEC and the movement of the CNA

If the CNA is at the location of NA, the criterion takes the form:

$$\sum F_{ic} + \sum F_{it} = 0 \tag{23}$$

Then,

$$\sum \sigma_{ic}a_{ic} + \sum \sigma_{it}a_{it} = 0 \tag{24}$$

where σ_{ic} is the stress of the compressive units, σ_{it} the stress of the tensile units, a_{ic} the area of the compressive units, and a_{it} the area of the tensile units.

If the distance between the NA and the CNA is Δz, the result ΔP_1 for the FEC is:

$$\begin{aligned}\Delta P_1 &= \frac{\sum F_{ic1}+\sum F_{it1}}{\sum F_{ic1}-\sum F_{it1}} \\ &= \frac{\sum \sigma_{ic1}a_{ic}+\sum \sigma_{it1}a_{it}}{\sum \sigma_{ic1}a_{ic}-\sum \sigma_{it1}a_{it}} \\ &= \frac{\sum \left(\sigma_{ic}+E_{iTc1}\Delta z\right)a_{ic}+\sum \left(\sigma_{it}+E_{iTt1}\Delta z\right)a_{it}}{\sum \left(\sigma_{ic}+E_{iTc1}\Delta z\right)a_{ic}-\sum \left(\sigma_{it}+E_{iTt1}\Delta z\right)a_{it}} \\ &= \frac{\Delta z\left(\sum E_{iTc1}a_{ic}+\sum E_{iTt1}a_{it}\right)}{\sum F_{ic}-\sum F_{it}+\Delta z\left(\sum E_{iTc1}a_{ic}-\sum E_{iTt1}a_{it}\right)}\end{aligned} \tag{25}$$

where E_{iTc1} and E_{iTt1} are the tangent moduli of the compressive or tensile unit i corresponding to the CNA.

Because,

$$\Delta z\left(\sum E_{iTc1}a_{ic}-\sum E_{iTt1}a_{it}\right)=\sum F_{ic}-\sum F_{it} \tag{26}$$

Therefore the ratio k_{P1} is:

$$k_{P1}=\frac{\Delta P_1}{\Delta z}\approx\frac{\left(\sum E_{iTc1}a_{ic}+\sum E_{iTt1}a_{it}\right)}{\sum F_{ic}-\sum F_{it}} \tag{27}$$

Eq. (27) shows that the relationship between the tolerance of the FEC and the movement of NA is approximately linear.

(2) Relationship between the rotation of the CNA and the result of the FEC

If the angle between the NA and the CNA is $\Delta\theta$, the result ΔP_2 for the FEC is:

$$\begin{aligned}\Delta P_2 &= \frac{\sum F_{ic1}+\sum F_{it1}}{\sum F_{ic1}-\sum F_{it1}} \\ &= \frac{\sum \sigma_{c1}a_{c}+\sum \sigma_{t1}a_{t}}{\sum \sigma_{c1}a_{c}-\sum \sigma_{t1}a_{t}} \\ &= \frac{\sum \left(\sigma_{c}+E_{Tc1}\Delta\theta\right)a_{c}+\sum \left(\sigma_{t}+E_{Tt1}\Delta\theta\right)a_{t}}{\sum \left(\sigma_{c}+E_{Tc1}\Delta\theta\right)a_{c}-\sum \left(\sigma_{t}+E_{Tt1}\Delta\theta\right)a_{t}} \\ &= \frac{\Delta\theta\left(\sum E_{Tc1}a_{c}+\sum E_{Tt1}a_{t}\right)}{\sum F_{ic}-\sum F_{it}+\Delta\theta\left(\sum E_{Tc1}a_{c}-\sum E_{Tt1}a_{t}\right)}\end{aligned} \tag{28}$$

Because,

$$\Delta\theta\left(\sum E_{Tc1}a_{c}-\sum E_{Tt1}a_{t}\right)=\sum F_{ic}-\sum F_{it} \tag{29}$$

Therefore, the ratio k_{P2} is:

$$k_{P2}=\frac{\Delta P_2}{\Delta\theta}\approx\frac{\left(\sum E_{Tc1}a_{c}+\sum E_{Tt1}a_{t}\right)}{\sum F_{ic}-\sum F_{it}} \tag{30}$$

Eq. (30) shows that the relationship between the tolerance of the FEC and the rotation of NA is approximately linear.

(3) Relationship between the translation of the CNA and the result of the IFVEC

If the CNA is at the location of NA, then the IFVEC takes the form:

$$y_c-y_t=0 \tag{31}$$

Therefore,

$$\frac{\sum F_{ic} y_i}{\sum F_{ic}} - \frac{\sum F_{it} y_i}{\sum F_{it}} = 0 \tag{32}$$

Then,

$$\sum \sigma_c a_c y_c \sum \sigma_t a_t - \sum \sigma_t a_t y_t \sum \sigma_c a_c = 0 \tag{33}$$

If the distance between the NA and the CNA is Δz, the result Δs_1 for the FVEC corresponding to the CNA is:

$$\begin{aligned} \Delta s_1 &= \frac{\sum \sigma_{c1} a_c y_c}{\sum \sigma_{c1} a_c} - \frac{\sum \sigma_{t1} a_t y_t}{\sum \sigma_{t1} a_t} \\ &= \frac{\sum (\sigma_c + E_{Tc1} \Delta z) a_c y_c}{\sum (\sigma_c + E_{Tc1} \Delta z) a_c} - \frac{\sum (\sigma_t + E_{Tt1} \Delta z) a_t y_t}{\sum (\sigma_t + E_{Tt1} \Delta z) a_t} \end{aligned} \tag{34}$$

Then,

$$\begin{aligned} \Delta s_1 / \Delta z &= (\sum \sigma_c a_c y_c \sum E_{Tt1} a_t + \sum E_{Tc1} a_c y_c \sum \sigma_t a_t + \Delta z \sum E_{Tc1} a_c y_c \sum E_{Tt1} a_t \\ &\quad - \sum \sigma_c a_c \sum E_{Tt1} a_t y_t - \sum E_{Tc1} a_c \sum \sigma_t a_t y_t - \Delta z \sum E_{Tc1} a_c \sum E_{Tt1} a_t y_t) / \\ &\quad (\sum \sigma_c a_c \sum \sigma_t a_t + \Delta z \sum \sigma_c a_c \sum E_{Tt1} a_t + \\ &\quad \Delta z \sum E_{Tc1} a_c \sum \sigma_t a_t + \Delta z^2 \sum E_{Tc1} a_c \sum E_{Tt1} a_t) \end{aligned} \tag{35}$$

Because $\Delta z E_T$ is much less than σ, the ratio k_{s1} is:

$$\Delta z E_T = \sigma \tag{36}$$

Then,

$$\begin{aligned} k_{s1} &= \frac{\Delta s_1}{\Delta z} \\ &\approx (\sum \sigma_c a_c y_c \sum E_{Tt1} a_t + \sum E_{Tc1} a_c y_c \sum \sigma_t a_t - \sum \sigma_c a_c \sum E_{Tt1} a_t y_t \\ &\quad - \sum E_{Tc1} a_c \sum \sigma_t a_t y_t) / \sum F_c \sum F_t \end{aligned} \tag{37}$$

Eq.(37) shows that the relationship between the result of the IFVEC and the movement of NA is approximately linear.

(4) Relationship between the rotation of the tolerance of the CNA and the IFVEC

If the rotation of the CNA is $\Delta\theta$, then the result Δs_2 for the IFVEC is:

$$\begin{aligned} \Delta s_2 &= \frac{\sum \sigma_{c1} a_c y_c}{\sum \sigma_{c1} a_c} - \frac{\sum \sigma_{t1} a_t y_t}{\sum \sigma_{t1} a_t} \\ &= \frac{\sum (\sigma_c + E_{Tc1} \Delta\theta) a_c y_c}{\sum (\sigma_c + E_{Tc1} \Delta\theta) a_c} - \frac{\sum (\sigma_t + E_{Tt1} \Delta\theta) a_t y_t}{\sum (\sigma_t + E_{Tt1} \Delta\theta) a_t} \end{aligned} \tag{38}$$

and,

$$\begin{aligned} \Delta s_2 / \Delta\theta &= (\sum \sigma_c a_c y_c \sum E_{Tt1} a_t + \sum E_{Tc1} a_c y_c \sum \sigma_t a_t + \Delta z \sum E_{Tc1} a_c y_c \sum E_{Tt1} a_t \\ &\quad - \sum \sigma_c a_c \sum E_{Tt1} a_t y_t - \sum E_{Tc1} a_c \sum \sigma_t a_t y_t - \Delta z \sum E_{Tc1} a_c \sum E_{Tt1} a_t y_t) \\ &\quad / (\sum \sigma_c a_c \sum \sigma_t a_t + \Delta z \sum \sigma_c a_c \sum E_{Tt1} a_t + \Delta z \sum E_{Tc1} a_c \sum \sigma_t a_t \\ &\quad + \Delta z^2 \sum E_{Tc1} a_c \sum E_{Tt1} a_t) \end{aligned} \tag{39}$$

Because,

$$\Delta\theta E_T = \sigma \tag{40}$$

The ratio k_{s2} is:

$$\begin{aligned} k_{s2} &= \frac{\Delta s_2}{\Delta\theta} \\ &= \frac{\sum \sigma_c a_c y_c \sum E_{Tt1} a_t + \sum E_{Tc1} a_c y_c \sum \sigma_t a_t - \sum \sigma_c a_c \sum E_{Tt1} a_t y_t - \sum E_{Tc1} a_c \sum \sigma_t a_t y_t}{\sum F_c \sum F_t} \end{aligned} \tag{41}$$

Eq.(41) shows that the relationship between the tolerance of the IFVEC and the rotation of NA is approximately linear.

4. Method verification

4.1 Verification model

To verify the relationship between the location of NA and the equilibrium criteria, the VLCC model used by ISSC (Yao et al, 2000), as shown in Fig. 7, is used for verification. The parameters of the stiffeners are shown in Table 1. The Young's module is 206GPa and the Poisson's ratio is 0.3.

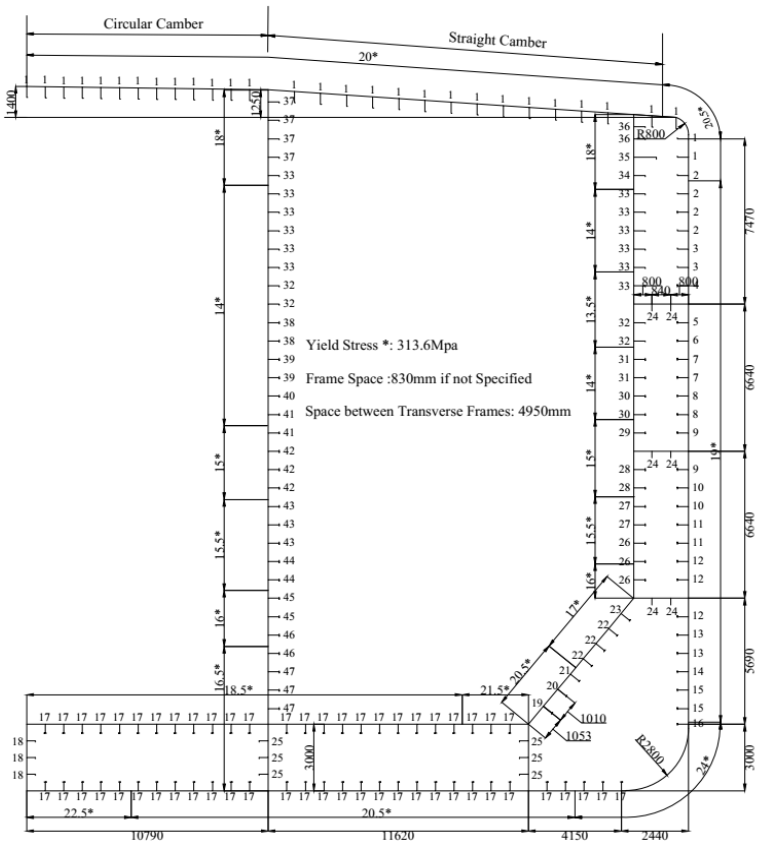

Fig. 7. Cross-section of the VLCC.

Table 1. Dimensions and materials of the stiffeners.

Stiffener ID	Dimensions (mm)	Type	Yield Stress (MPa)	Stiffener ID	Dimensions (mm)	Type	Yield Stress (MPa)
1	300 × 90 × 13/17 IA	Angle Bar	313.6	25	250 × 90 × 12/16 IA	Angle bar	313.6
2	350 × 100 × 12/17 IA	Angle Bar	313.6	26	450 × 11 + 150 × 22	T-bar	352.8
3	400 × 100 × 11.5/17 IA	Angle bar	313.6	27	450 × 11 + 150 × 19	T-bar	352.8
4	400 × 11 + 150 × 12	T-bar	313.6	28	450 × 11 + 150 × 16	T-bar	352.8
5	400 × 11 + 150 × 14	T-bar	313.6	29	450 × 11 + 150 × 14	T-bar	352.8
6	450 × 11 + 150 × 12	T-bar	313.6	30	450 × 11 + 150 × 12	T-bar	352.8
7	400 × 11 + 150 × 14	T-bar	313.6	31	450 × 11 + 150 × 14	T-bar	352.8
8	450 × 11 + 150 × 16	T-bar	313.6	32	400 × 100 × 11.5/16 IA	Angle bar	352.8
9	450 × 11 + 150 × 19	T-bar	313.6	33	350 × 100 × 12/17 IA	Angle bar	352.8
10	450 × 11 + 150 × 22	T-bar	313.6	34	300 × 90 × 13/17 IA	Angle bar	352.8
11	450 × 11 + 150 × 25	T-bar	313.6	35	850 × 17 + 150 × 19	Angle bar	352.8
12	500 × 11 + 150 × 28	T-bar	313.6	36	250 × 90 × 12/16 IA	Angle bar	352.8
13	500 × 11 + 150 × 30	T-bar	313.6	37	300 × 90 × 12/16 IA	Angle bar	352.8
14	500 × 11 + 150 × 32	T-bar	313.6	38	400 × 11 + 150 × 14	T-bar	352.8

15	500 × 11 + 150 × 34	T-bar	313.6	39	450 × 11 + 150 × 12	T-bar	352.8
16	550 × 12 + 150 × 30	T-bar	313.6	40	450 × 11 + 150 × 14	T-bar	352.8
17	550 × 12 + 150 × 25	T-bar	313.6	41	450 × 11 + 150 × 16	T-bar	352.8
18	350 × 100 × 12/17 IA	Angle bar	313.6	42	450 × 11 + 150 × 19	T-bar	352.8
19	550 × 12.5 + 150 × 32	T-bar	352.8	43	450 × 11 + 150 × 22	T-bar	352.8
20	500 × 11.5 + 150 × 30	T-bar	352.8	44	450 × 11 + 150 × 25	T-bar	352.8
21	500 × 11.5 + 150 × 28	T-bar	352.8	45	450 × 11 + 150 × 28	T-bar	352.8
22	500 × 11 + 150 × 25	T-bar	352.8	46	500 × 11 + 150 × 25	T-bar	352.8
23	450 × 11 + 150 × 28	T-bar	352.8	47	500 × 11 + 150 × 28	T-bar	352.8
24	250 × 12.5	Flat bar	313.6	48	230 × 12.5	Flat bar	313.6

To study the movement of NA of the asymmetric cross-section, the damage parameters given in the HCSR are adopted. The damage location is shown in Fig. 8, and the damage parameters are given in Table 2. B is the width of the ship, and D is the depth of the ship, and b is the width of the breakage, and d is the depth of the breakage.

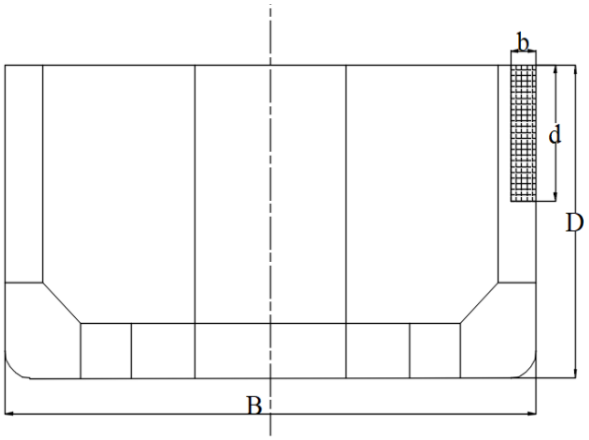

Fig. 8. Cross-section of the VLCC.

Table 2. Parameters of the damage.

Location	b	d
Length	$0.0625B$	$0.600D$

4.2 Verification results

The residual strength of the damaged ship is calculated by the linear search method, and the curvature-moment curve is shown in Fig. 9. It is found that the curvature-moment curve has 4 stages: Linear Stage (LS), NonLinear Stage (NLS), Ultimate Strength Stage (USS) and Post Ultimate Strength Stage (PUSS), respectively. To investigate the relationship between the results of the equilibrium criteria and the location of NA in different stages, 4 curvatures are chosen, namely, $2.01\times10^{-4}\mathrm{m}^{-1}$, $4.02\times10^{-4}\mathrm{m}^{-1}$, $6.90\times10^{-4}\mathrm{m}^{-1}$ and $8.00\times10^{-4}\mathrm{m}^{-1}$. For each stage, 11 heights are selected ranging from $z_j-0.025D$ to $z_j+0.025D$, and 11 angles are selected ranging from $\theta_j-1°$ to $\theta_j+1°$. z_j and θ_j are the height and angle of NA, respectively. The spacing of the two heights is $0.005D$ and the spacing of the two angles is $0.2°$. The results for the equilibrium criteria at every calculation point of different curvatures are shown in Figs. 10–17.

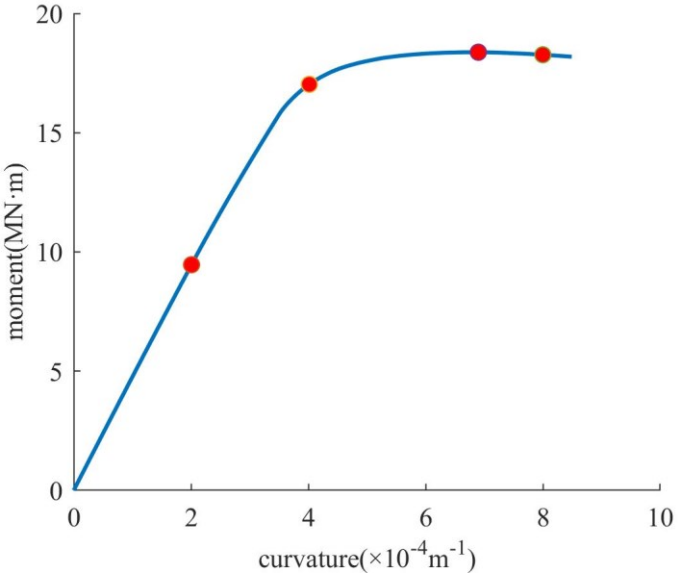

Fig. 9. Curvature-moment curve of the damaged ship.

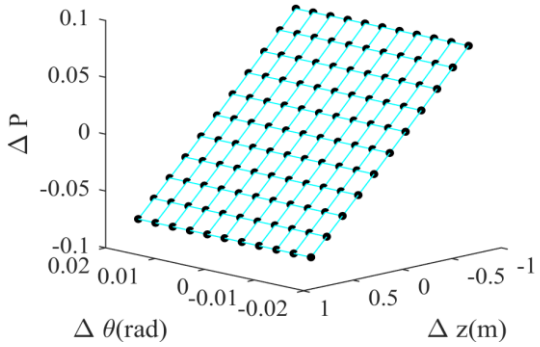

Fig. 10. Results for the FVC in the LS.

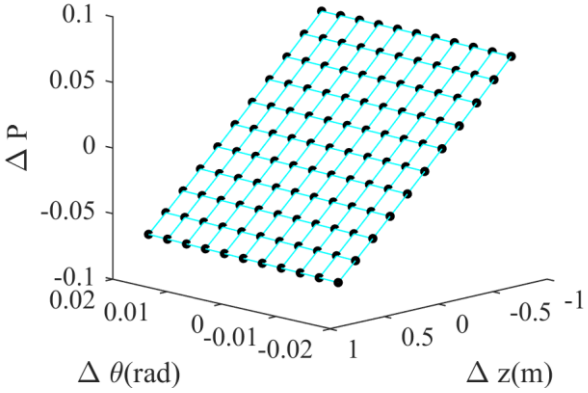

Fig. 11. Results for the FVC in the NLS.

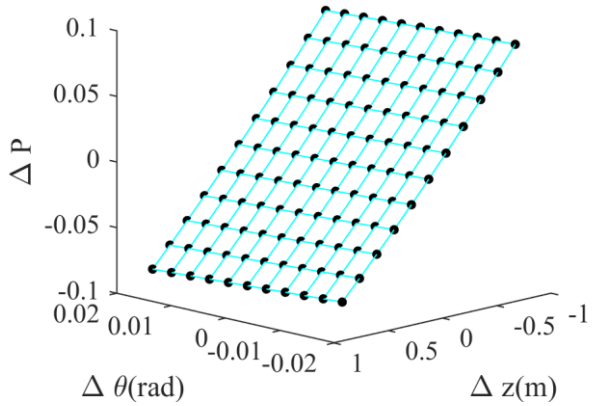

Fig. 12. Results for the FVC in the USS

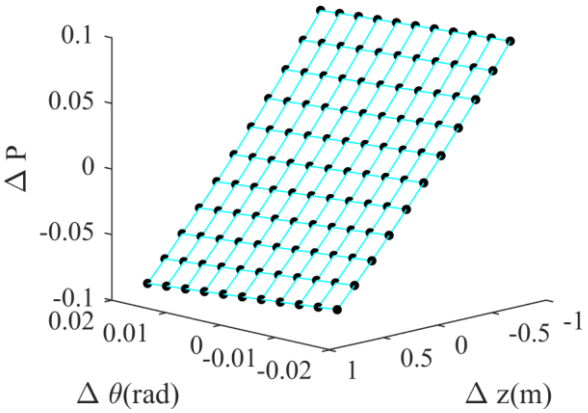

Fig. 13. Results for the FVC in the PUSS

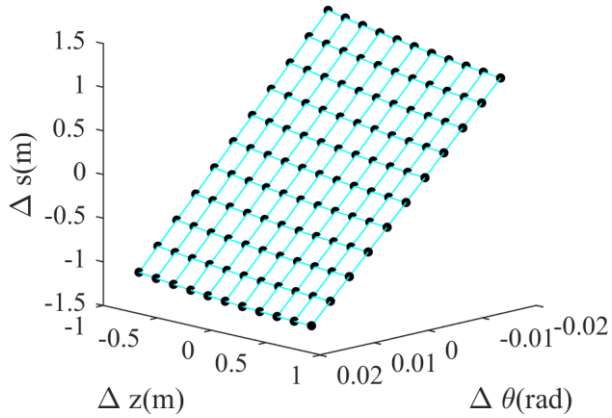

Fig. 14. Results for the IFVEC in the LS.

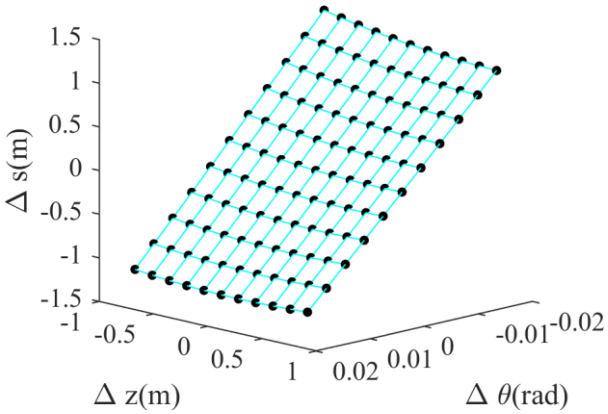

Fig. 15. Results for the IFVEC in the NLS.

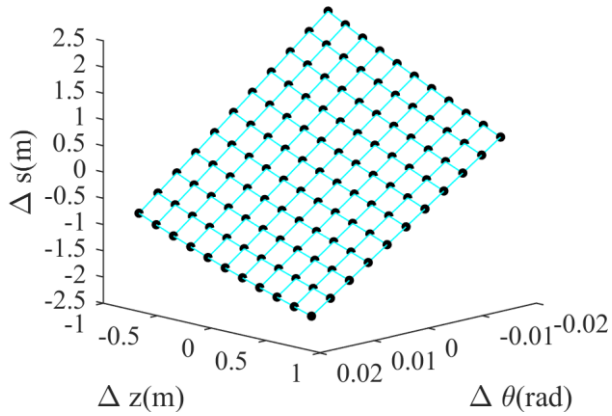

Fig. 16. Results for the IFVEC in the USS.

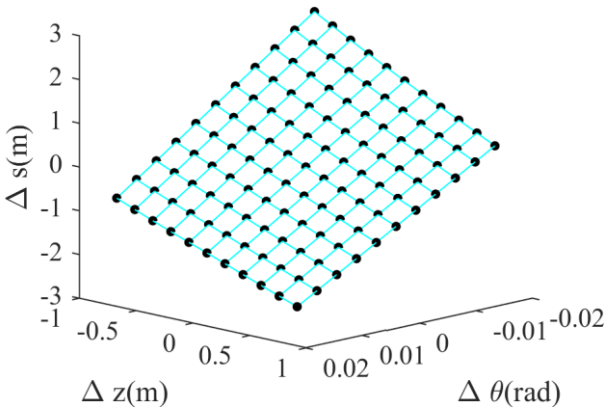

Fig. 17. Results for the IFVEC in the PUSS.

It is found that at each stage, the results for FEC and IFVEC approximately fall into the same planes, which suggests that the results of the criteria vary linearly with the translation or rotation of NA. As shown Figs. 10–13, the result for FEC ΔP varies significant with the height of NA, but little with the angle of NA. In Figs. 14–17, the IFVEC not only varies significantly with the height of NA, but also with the angle of NA. To verify that the criterion results vary linearly with the location of NA, a set of equations are adopted to fit the results:

$$\begin{cases} \Delta P = a_p \Delta z + b_p \Delta\theta + c_p \\ \Delta s = a_s \Delta z + b_s \Delta\theta + c_s \end{cases} \tag{42}$$

The parameters of the fitting equations and the goodness of fit are shown in Table 3.

Table 3. Parameters of the fitting equations and the goodness of fit.

Results	Stage	a	b	c	Goodness of fit
FEC	LS	-9.766×10^{-2}	-1.345×10^{-3}	5.186×10^{-4}	9.999×10^{-1}
	NLS	-8.857×10^{-2}	7.269×10^{-2}	5.645×10^{-4}	9.998×10^{-1}
	USS	-1.048×10^{-1}	-2.053×10^{-1}	1.681×10^{-3}	9.992×10^{-1}
	PUSS	-1.107×10^{-2}	-3.272×10^{-1}	2.402×10^{-3}	9.986×10^{-1}
IFVEC	LS	-1.525×10^{-1}	-69.362	1.351×10^{-2}	9.994×10^{-1}
	NLS	-8.539×10^{-2}	-67.901	2.234×10^{-2}	9.987×10^{-1}
	USS	-8.879×10^{-1}	-80.577	1.829×10^{-2}	9.977×10^{-1}
	PUSS	-1.174	-84.772	1.300×10^{-2}	9.971×10^{-1}

It is found in Table 3 that at each stage, the goodness of fit exceeds 0.99, so the surfaces formed by the criterion results in Figs. 10–17 can be considered as planes. According to the fitting formula, it is seen that within a suitable range, the relationship between the criterion results and the height of NA is linear, and the relationship between the results and the angle of NA is also linear, and these two relationships are independent. Comparing the fitting results for the FEC and the IFVEC, it can be seen that the influence of the change in angle on the results for IFVEC is much greater than that of the FEC. The fitting results of c are close to 0, and it is reasonable to assume that c is 0 in the equations.

In order to further analyze the results of formula derivation and fitting, the relationships between the results for the FEC and the movement of the CNA are calculated by Eq.(43) and the results are shown in Tables 4 and 5.

$$\begin{cases} k'_{p1} = \dfrac{\Delta P_1}{\Delta z} \\ k'_{p2} = \dfrac{\Delta P_2}{\Delta \theta} \end{cases} \tag{43}$$

where ΔP_1 and ΔP_2 are the results for the FEC when the CNA is near the NA, and Δz and $\Delta\theta$ are the changes in the height and in the angle respectively.

The relationships between the results for the IFVEC and the movement of NA are calculated by Eq. (44) and the results are shown in Table 6 and Table 7.

$$\begin{cases} k'_{s1} = \dfrac{\Delta s_1}{\Delta z} \\ k'_{s2} = \dfrac{\Delta s_2}{\Delta \theta} \end{cases} \tag{44}$$

where $\Delta s1$ and $\Delta s2$ are the results for the IFVEC when CNA is near NA, and Δz and $\Delta\theta$ are the changes in the height and in the angle respectively.

In Tables 4–7, the error γ between the ratio k and the ratio k' is calculated as:

$$\gamma = (k' - k)/k \tag{45}$$

The error γ' between the ratio k and the fitted parameter a or b is calculated as:

$$\begin{cases} \gamma' = (a - k)/k \\ \gamma' = (b - k)/k \end{cases} \tag{46}$$

Table 4. Ratios of the results for the relationship between the FEC and translation of NA.

Stage	k_{p1}	k'_{p1}	γ_{p1}	a_p	γ'_{p1}
LS	-9.806×10^{-2}	-9.806×10^{-2}	0.00%	-9.766×10^{-2}	−0.40%
NLS	-8.885×10^{-2}	-8.885×10^{-2}	0.00%	-8.857×10^{-2}	−0.31%
USS	-1.064×10^{-1}	-1.064×10^{-1}	0.00%	-1.048×10^{-1}	−1.37%
PUSS	-1.118×10^{-2}	-1.118×10^{-2}	0.00%	-1.107×10^{-2}	−0.83%

Table 5. Ratios of the results for the relationship between the FEC and rotation of NA.

Stage	k_{p2}	k'_{p2}	γ_{p2}	b_p	γ'_{p2}
LS	9.847×10^{-4}	9.848×10^{-4}	0.01%	-1.345×10^{-3}	36.59%
NLS	7.357×10^{-2}	7.357×10^{-2}	0.00%	7.269×10^{-2}	−1.20%
USS	-1.934×10^{-1}	-1.934×10^{-1}	0.00%	-2.053×10^{-1}	5.85%
PUSS	-3.340×10^{-1}	-3.340×10^{-1}	0.00%	-3.272×10^{-1}	−1.98%

Table 6. Ratios of the results for the relationship between the IFVEC and translation of NA.

Stage	k_{s1}	k'_{s1}	γ_{s1}	a_s	γ'_{s1}
LS	-1.598×10^{-1}	-1.598×10^{-1}	0.00%	-1.525×10^{-1}	−4.30%
NLS	-9.412×10^{-1}	-9.413×10^{-1}	0.01%	-8.539×10^{-2}	−8.13%
USS	-8.743×10^{-1}	-8.743×10^{-1}	0.00%	-8.879×10^{-1}	1.54%
PUSS	−1.200	−1.200	0.00%	−1.174	−2.17%

Table 7. Ratios of the results for the relationship between the IFVEC and rotation of NA.

Stage	k_{s2}	k'_{s2}	γ_{s2}	b_s	γ'_{s2}
LS	−69.412	−69.412	0.00%	−69.362	−0.07%
NLS	−67.907	−67.784	−0.18%	−67.901	−0.01%
USS	−81.023	−81.021	0.00%	−80.577	−0.55%
PUSS	−84.233	−84.230	0.00%	−84.772	0.64%

The ratio k derived from the formula (namely, Eq.(20), Eq.(30), Eq.(37) and Eq.(41)), the ratio k' calculated by Eq.(43) and Eq.(44) , and the coefficients a and b calculated by fitting are shown in Tables 4−7. The error γ shows that k and k' are so close that the difference is negligible, which indicates that the derived formula is accurate. by comparing k with a or b, it is found that the error γ' is small, as shown in Table 4 and Table 7, while the error is significant in Table 5 and Table 6. It is shown that the relationship between the translation of NA and the result of the FEC, and the relationship between the rotation of the neutral axis and the result of the IFVEC are more 'linear' than the other two relationships.

The results of the criteria at different locations of the CNA are obtained by Eq.(47) and Eq.(48).

$$P = k'_{p1}z + k'_{p2}\theta \tag{47}$$

$$s = k'_{s1}z + k'_{s2}\theta \tag{48}$$

Then the errors between these results and the results calculated by the criteria are shown in Figs. 18−25.

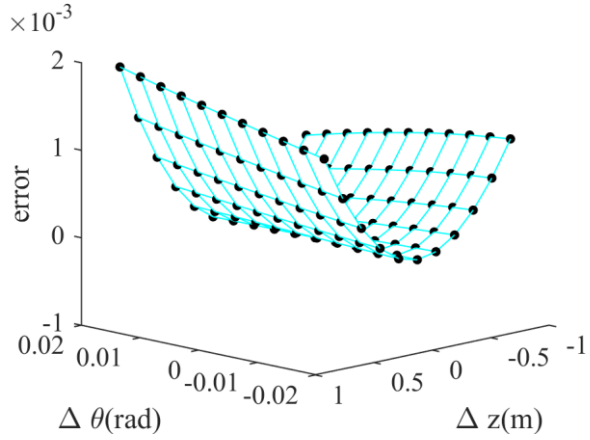

Fig. 18. Errors of FEC in the LS.

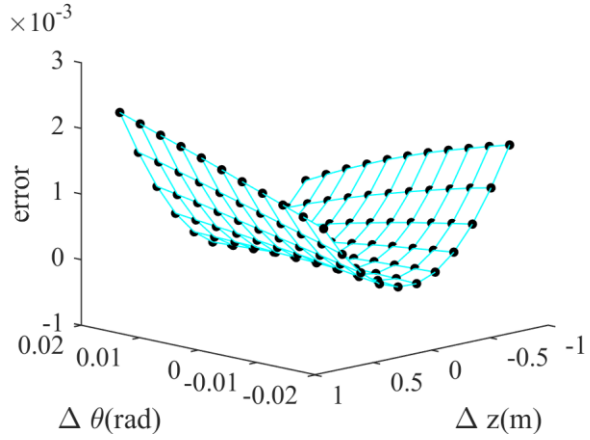

Fig. 19. Errors of FEC in the NLS.

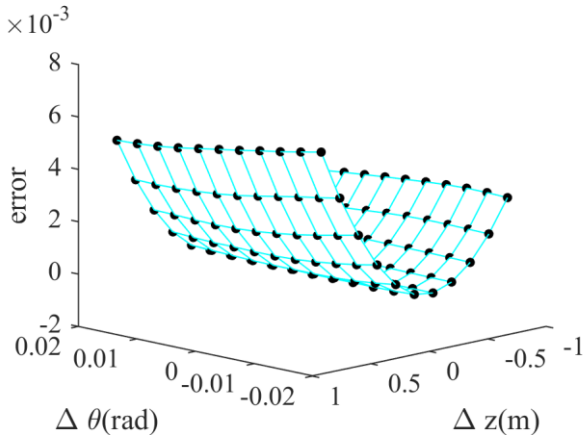

Fig. 20. Errors of FEC in the USS.

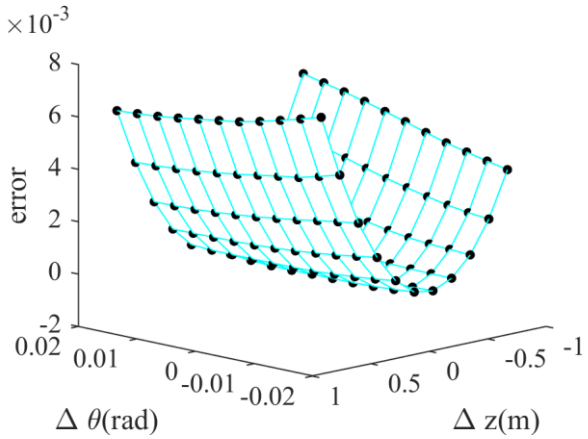

Fig. 21. Errors of FEC in the PUSS.

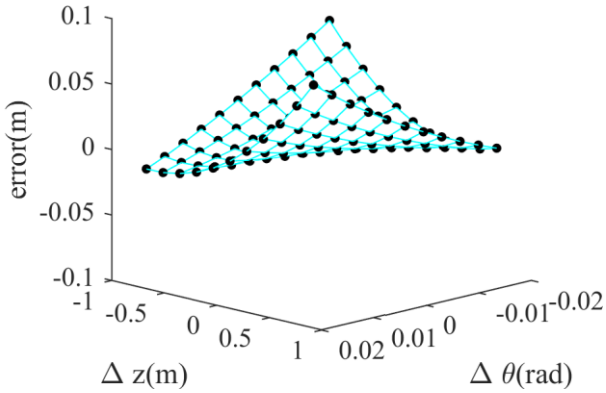

Fig. 22. Errors of IFVEC the in LS.

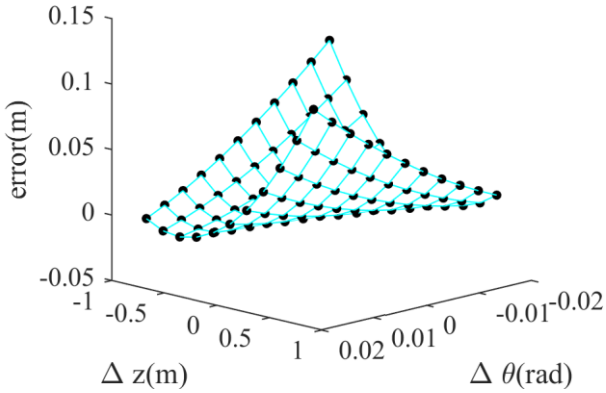

ig. 23. Errors of IFVEC in the NLS.

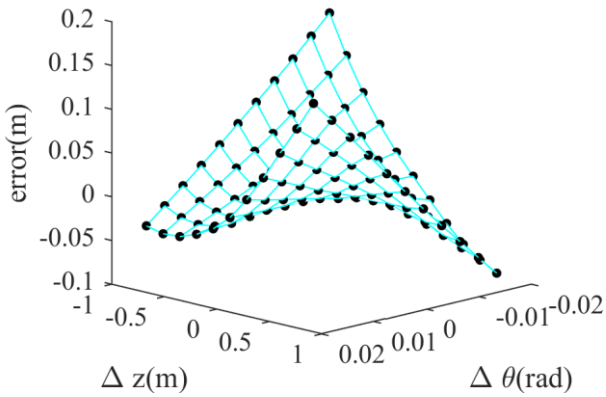

Fig. 24. Errors of IFVEC in the USS.

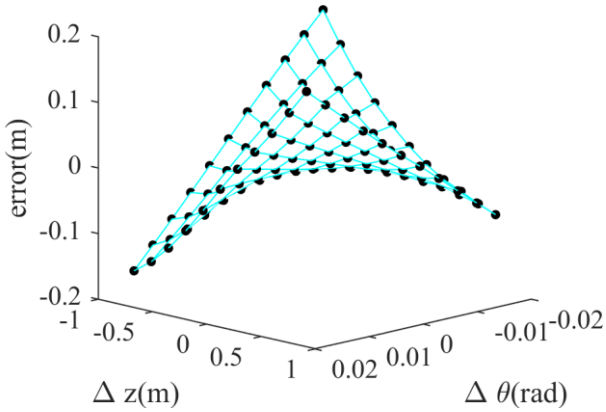

Fig. 25. Errors of IFVEC in the PUSS.

Figs. 18–25 show that the error of criterion results varies with the height and angle of NA. They also show that the errors become greater when the movement is larger, and the change is also nonlinear. Figs. 18–21 show that the surface formed by errors of the FEVC is U-shaped, but the errors barely change with the angle of NA. Compared to the results presented in Figures 10–13, the errors are relatively small. Figs. 22–25 show that the errors of the IFVEC change nonlinearly with the movement of NA and become significant when NA moves. Compared to the results for the IFVEC, the errors are also small. If the movement of NA is small, the errors are also small compared to the results calculated by the criteria. Therefore, the results of the criteria and the movement of NA have a linear relationship for a small range of translation and rotation. The linear relationships are shown as follows:

$$\begin{cases} P_1 = k_{p1} z \\ P_2 = k_{p2} \theta \end{cases} \tag{49}$$

$$\begin{cases} s_1 = k_{s1} z \\ s_2 = k_{s2} \theta \end{cases} \tag{50}$$

Although the ratio k can be calculated by the derived method, the method is not practically useful because the location of the CNA is unknown. A reasonable method should be one that can obtain two criteria results for two CNAs near NA. Then the ratio k is calculated by the two locations and the two results. If the angles are the same, the heights are z_1 and z_2, and the results of the FEC are P_{11} and P_{12}, then the ratio k can be obtained

$$k_{p1} = \frac{P_{21} - P_{11}}{z_2 - z_1} \tag{51}$$

A good choice of the locations of the CNA is the two sides of NA. If the change in the curvature is small, so will be the movement of NA. Therefore, the locations of CNAs can be selected on both sides of the location of NA at the last curvature, whose height is z_{j-1} and angle is θ_{j-1}, and the appropriate height increment Δz and angle increment $\Delta\theta$ can determined to obtain the locations of the CNAs for this curvation. For the two CNAs that have the same angle θ_{j-1} but different heights ($z_{j-1} - \Delta z$ and $z_{j-1} + \Delta z$, respectively), the results for P_{j1} and P_{j2} can be obtained by the FEC, and that for s_{j1} and s_{j2} by IFVEC. For the two CNAs that have the same height z_{j-1} but different angles ($\theta_{j-1} - \Delta\theta$ and $\theta_{j-1} + \Delta\theta$), the results for P_{j3}, P_{j4}, s_{j3} and s_{j4} can also be obtained using the same criteria respectively. The iterative processes of the calculation of CNAs are continued until the results of criterion equations reach zero. These two processes, namely (1) the same height but different angles and (2) the same angle but different heights, will result in two NAs, and there locations can be calculated as:

$$z_j = z_{j-1} - \Delta z - \frac{P_{1j1}}{k_{P1j}} \tag{52}$$

$$\theta_j = \theta_{j-1} - \Delta\theta - \frac{P_{2j1}}{k_{p2j}} \tag{53}$$

$$z'_j = z_{j-1} - \Delta z - \frac{s_{1j1}}{k_{s1j}} \tag{55}$$

$$\theta'_j = \theta_{j-1} - \Delta\theta - \frac{s_{2j1}}{k_{s2j}} \tag{54}$$

Since there are two heights and two angles of NA, it is necessary to find out which are more accurate, and discuss the influence of the locations of CNA. The results of the criteria under different combinations of the range of angle and the range of height of CNA are obtained and compared. The errors are shown in Figs.26–41.

In Figs.26–29, it can be seen that the error of the height of NA changes little with the decrease of the range of the angle, and the errors are in general small, i.e. samller than 0.03m. Figs.30–33 show that the errors is very small over the range of $\Delta\theta$, while it changes ripidly with the height Δz. Comparison of Figs.26–33 shows that when the FEC is adopted to obtain the location of NA, the results for the height calculated by the linear equation are accurate and barely affected by the the translation and rotation of NA. However, the accuracy of the results for the angle is poor and affected by the height of the CNA, as shown in Figs.30–33.

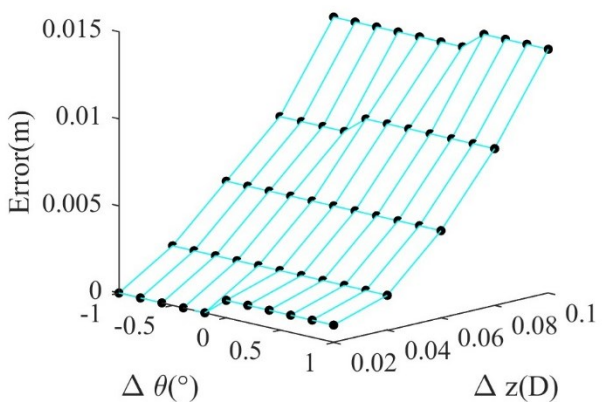

Fig.26. Errors of the height of NA based on the FEC in the LS.

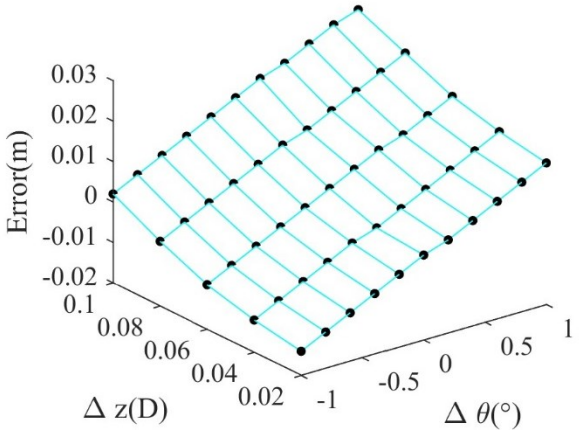

Fig.27. Errors of the height of NA based on the FEC in the NLS.

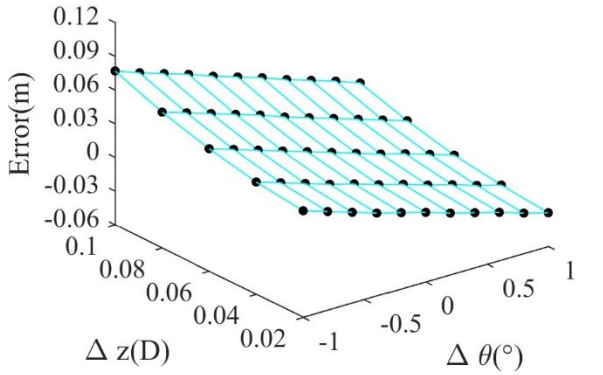

Fig.28. Errors of the height of NA based on the FEC in the USS.

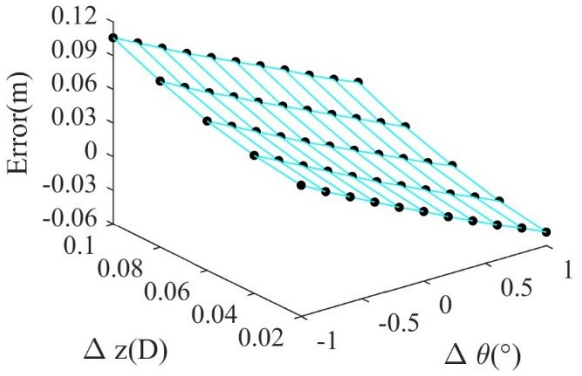

Fig.29. Errors of the height of NA based on the FEC in the PUSS.

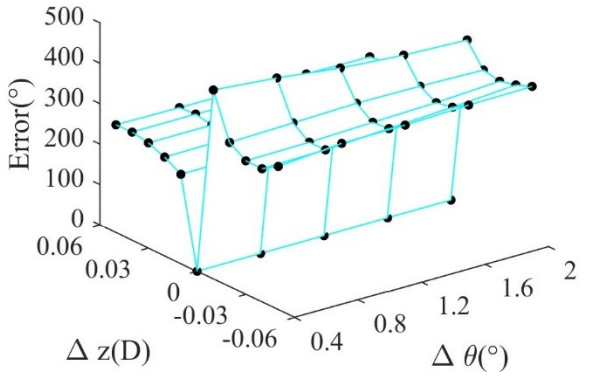

Fig.30. Errors of the angle of NA based on the FEC in the LS.

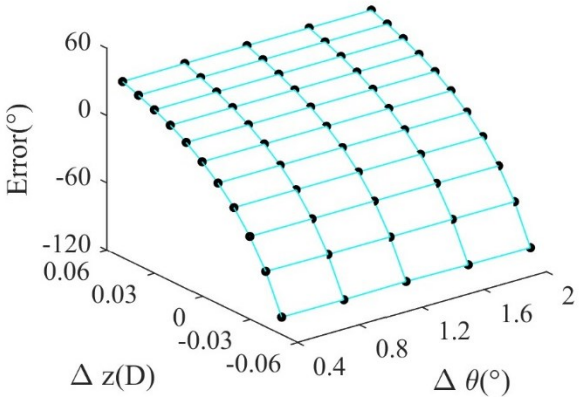

Fig.31. Errors of the angle of NA based on the FEC in the NLS.

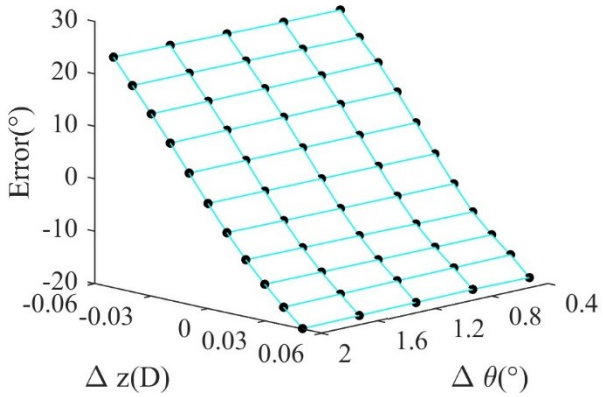

Fig.32. Errors of the angle of NA based on the FEC in the USS.

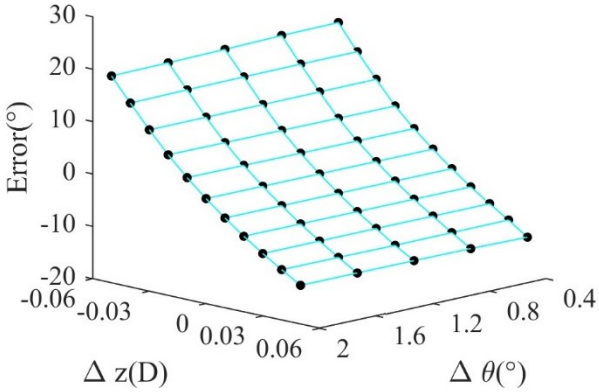

Fig.33. Errors of the angle of NA based on the FEC in the PUSS.

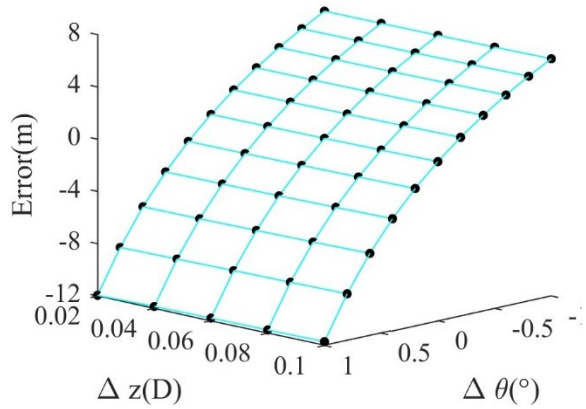

Fig.34. Errors of the height of NA based on the IFVEC in the LS.

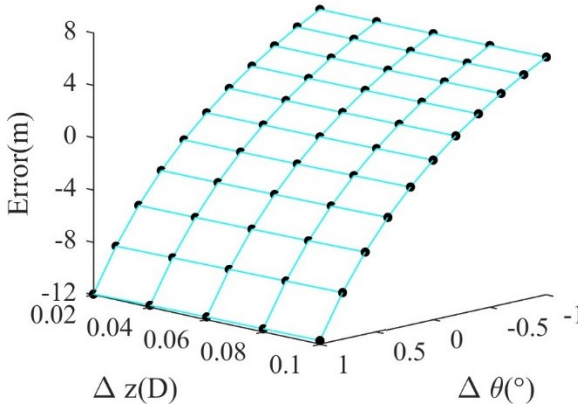

Fig.35. Errors of the height of NA based on the IFVEC in the NLS.

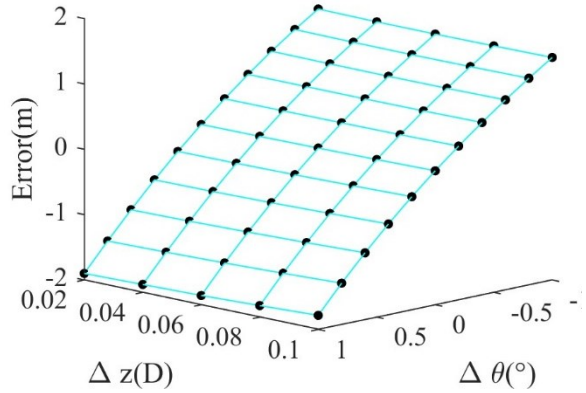

Fig.36. Errors of the height of NA based on the IFVEC in the USS.

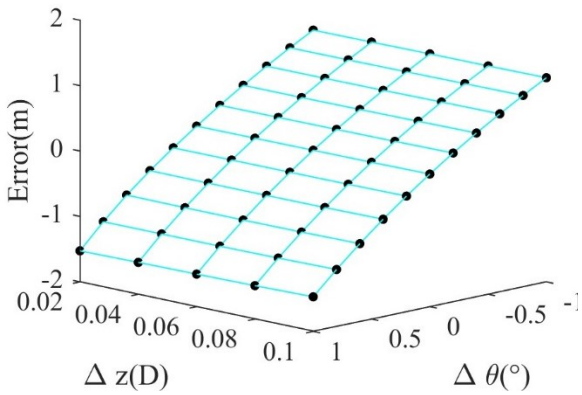

Fig.37. Errors of the height of NA based on the IFVEC in the PUSS.

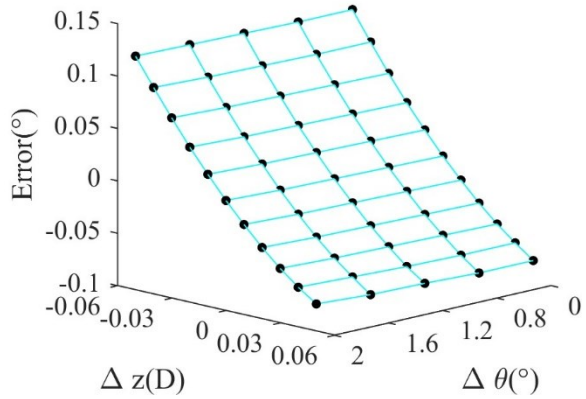

Fig.38. Errors of the angle of NA based on the IFVEC in the LS.

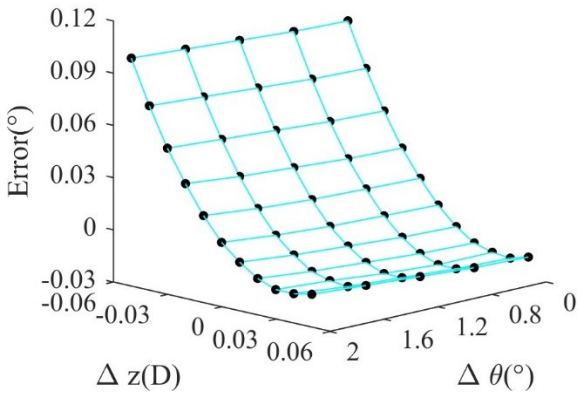

Fig.39. Errors of the angle of NA based on the IFVEC in the NLS.

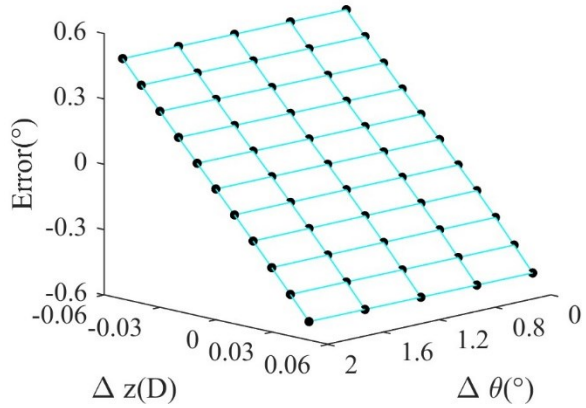

Fig.40. Errors of the angle of NA based on the IFVEC in the USS.

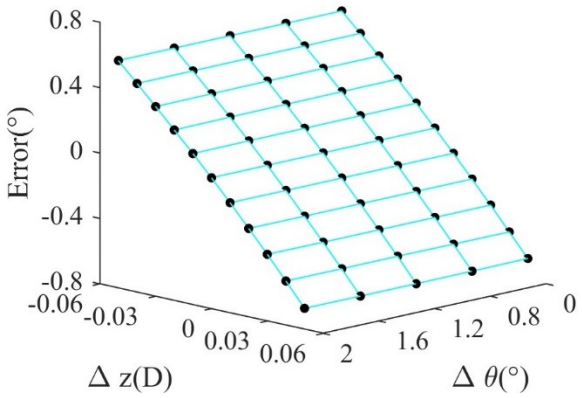

Fig.41. Errors of the angle of NA based on the IFVEC in the PUSS.

In Figs. 34–37, it can be seen that the error merely varies with the height of NA, but rapidly with $\Delta\theta$. It is also found that when the angle of CNA is close to the location of NA, the errors of the height are small. The larger is the deviation of the angle, the larger are the errors of the height. Similar patterns are also observed in Figs.38–41. Comparison of Figs.34–41 show that when the IFVEC is adopted to obtain the location of NA, the accuracy of the results is good for the angle of NA, but poor for the height of NA.

The results show that the FEC is accurate for the height of NA, and the influences of the height and the range of the angle of NA are small. The IFVEC is accurate for the angle of NA, because the influence of the range of angle is small. This observation is consistent with the findings of existing studies (Choung et al., 2012; Choung et al., 2014) that: the FEC is recommended for the search of the height of NA and the IFVEC for the angle. Therefore, the FEC and Eq.(52) can be adopted to obtain the height of NA, and the IFVEC and Eq.(54) the angle of NA.

In the calulation with the iterative method for the height and angle, tolerances are specified to achieve the best tradeoff between efficiency and accuracy (Choung et al, 2012; Choung, 2014). The tolerance can be set to 0.1m for the height and 0.1° for the angle. The results of the FEC and IFVEC are shown in Table 8 and Table 9.

Table 8. Results of the FEC obtained with the recommended tolerance for the height.

Stage	Height	−0.1°	0.0°	0.1°
LS	−0.1m	9.80×10^{-3}	9.79×10^{-3}	9.79×10^{-3}
	0m	1.43×10^{-6}	0	-1.51×10^{-6}
	0.1m	-9.75×10^{-3}	-9.75×10^{-3}	-9.75×10^{-3}
NLS	−0.1m	8.80×10^{-3}	8.84×10^{-3}	8.89×10^{-3}
	0m	-5.53×10^{-5}	0	5.56×10^{-5}
	0.1m	-8.85×10^{-3}	-8.78×10^{-3}	-8.72×10^{-3}
USS	−0.1m	9.93×10^{-3}	9.71×10^{-3}	9.49×10^{-3}
	0m	2.09×10^{-4}	0	-2.14×10^{-4}
	0.1m	-9.43×10^{-3}	-9.64×10^{-3}	-9.84×10^{-3}
PUSS	−0.1m	1.02×10^{-2}	9.96×10^{-3}	9.72×10^{-3}
	0m	2.47×10^{-4}	0	-2.47×10^{-4}
	0.1m	-9.61×10^{-3}	-9.85×10^{-3}	-1.01×10^{-2}

Table 9. Results of the IFVEC obtained with the recommended tolerance for the height.

Stage	Height	−0.1°	0.0°	0.1°
LS	−0.1m	1.37×10^{-1}m	1.55×10^{-2}m	-1.06×10^{-1}m
	0m	1.21×10^{-1}m	0m	-1.21×10^{-1}m
	0.1m	1.05×10^{-1}m	-1.47×10^{-2}m	-1.35×10^{-1}m
NLS	−0.1m	1.41×10^{-1}m	2.08×10^{-2}m	-9.97×10^{-2}m
	0m	1.20×10^{-1}m	0m	-1.20×10^{-1}m
	0.1m	1.00×10^{-1}m	-1.92×10^{-2}m	-1.38×10^{-1}m
USS	−0.1m	1.98×10^{-1}m	6.63×10^{-2}m	-6.57×10^{-2}m
	0m	1.31×10^{-1}m	0m	-1.31×10^{-1}m
	0.1m	6.66×10^{-2}m	-6.36×10^{-2}m	-1.94×10^{-1}m
PUSS	−0.1m	2.07×10^{-1}m	7.22×10^{-2}m	-6.30×10^{-2}m
	0m	1.34×10^{-1}m	0m	-1.34×10^{-1}m
	0.1m	6.26×10^{-2}m	-7.06×10^{-2}m	-2.04×10^{-1}m

Table 8 and Table 9 show that the smallest result of the FEC is 8.80×10^{-3} and the smallest result of the IFVEC is 6.26×10^{-2}m when the height and the angle reach the range of the boundaries of the ranges. Therefore, a convergence factor δ_1 of the FEC can be set to a threshold

that is smaller than $8.80\times10^{-3,}$ to a 5×10^{-3} and the convergence factor δ_2 of the IFVEC is 5×10^{-2}m.

4.3 Calculation process of the improved Smith method

Based on the derivations and analysis of results, an Improved Smith method is proposed and applied to the asymmetric cross-section, which is also referred to as the Smith method based on the linear equation. The calculation process is:

(1) Divide the cross-section into stiffener plate units, plate units, and hard corner units;

(2) Define the stress-strain relationships for all types of units;

(3) Initialize the curvature and the NA, and the height of NA denoted by z_{j-1} and the angle by θ_{j-1};

(4) Increase the curvature and select two calculation neutral axes N_{j1} and N_{j2}, with their heights being $z_{j-1}+\Delta z$ and $z_{j-1}-\Delta z$, and their angle θ_{j-1};

(5) Calculate the FEC results P_{j1} and P_{j2} for the two calculation neutral axes N_{j1} and N_{j2};

(6) Calculate the height z_j of NA— N_j using

$$z_j=\frac{P_{j1}(z_{j-1}+\Delta z)-P_{j2}(z_{j-1}-\Delta z)}{P_{j1}-P_{j2}} \tag{55}$$

(7) Select two calculation neutral axes N_{j3} and N_{j4}, which have the same height z_j, but different angles: respectively $\theta_{j-1}-\Delta\theta$ and $\theta_{j-1}+\Delta\theta$;

(8) Calculate the IFVEC results for s_{j1} and s_{j1} for the two calculation neutral axes N_{j3} and N_{j4};

(9) Calculate the angle θ_j of NA N_j by:

$$\theta_j=\frac{s_{j1}(\theta_{j-1}+\Delta\theta)-s_{j2}(\theta_{j-1}-\Delta\theta)}{s_{j1}-s_{j2}} \tag{56}$$

(10) Calculate the FEC result for P_j and the IFVEC result for s_j of NA, if the results satisfy the criteria, go to Step (12), otherwise change the initial height of NA to z_j and the initial angle to θ_j, and then go to Step 5;

(11) Calculate the sum of the unit moments, and obtain the bending moment of the cross-section;

(12) Compare the moment in the current incremental step with the previous one. If the slope in the M-χ relationship is smaller than a negative fixed value, terminate the process and define the peak value of M_U. Otherwise, increase the curvature by the amount of $\Delta\chi$ and go to Step (4).

The flowchat of the calculation process is shown in Fig.42.

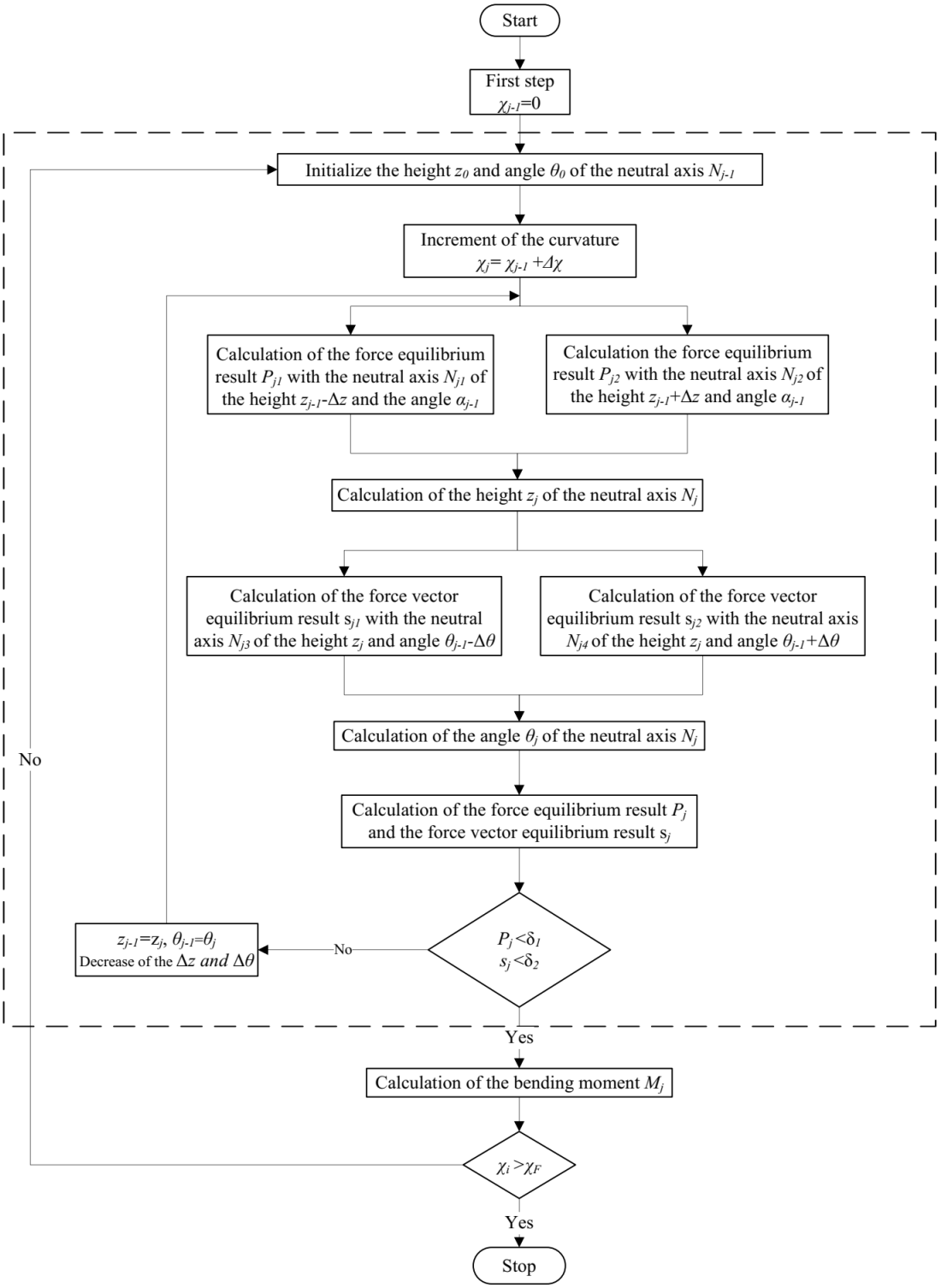

Fig. 42. Calculation process of the linear-based Smith method.

4.4 Assessment of the longitudinal strength

The results calculated by the Improved Smith method based on the linear equation for the intact VLCC, and the results given by ISSC (2000; 2012) and Li et al (2017; 2018) are shown in Table 10. The residual longitudinal strength of the damaged ship calculated by the Improved Smith method based on the linear search (Method 1), the improved Smith method based on the PSO (Method 2) and the Improved Smith method based on the linear equation (Method 3) and

the results are shown in Table 11. The bending moments, the height and the angle of NA of the damaged hull are shown in Fig. 43.

Table 10. Results for the ultimate strength.

Source	Contributor	Methodology	Ultimate Strength (MN·m)	
			Hogging	Sagging
ISSC 2000 Report [Yao et al., 2000]	Chen	ISUM	27.40	24.33
	Cho	Smith Method	28.66	20.80
	Yao	Smith Method	28.88	20.42
	Rigo (1)	Smith Method	28.31	19.57
	Rigo (2)	Modified P-M	25.61	24.07
	Masaoka	ISUM	30.59	26.59
ISSC 2012 Report [Paik et al., 2012]	Paik	NLFEA	27.34	22.50
		ISUM	25.59	21.97
		Modified P-M	25.67	22.39
		Smith	28.42	22.13
	Wang	NLFEA	31.00	25.00
		Smith	29.85	25.01
	UoG	RINA Rules	28.20	21.70
Li *et al.*(2017)		The linear search method	29.20	21.90
Li *et al.*(2018)		PSO-based Smith	29.20	21.90
Present study		The linear equation method	**29.20**	**21.90**

Table 11. Comparison of results for the residual strength

Methodology	Sagging (MN·m)	Hogging (MN·m)
Method 1	23.92	17.41
Method 2	23.92	17.41
Method 3	23.92	17.41

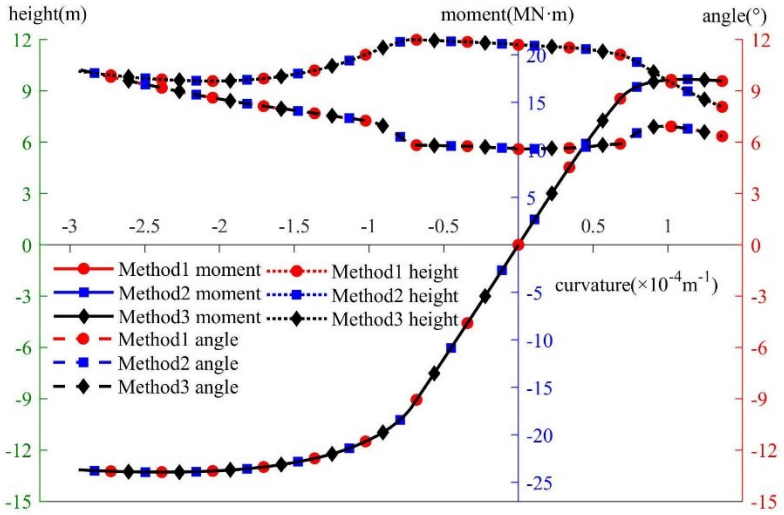

Fig. 43. Comparison of results of different calculation methods.

Table 12 shows that the results calculated by Method 3 are approximately the same as those calculated by Method 1 and Method 2, and the comparison of the results with the ISSC ones shows that the accuracy of the results is satisfying. It can be seen in Fig. 43 that the angle curve, the height curve and the moment curve of the results by the three methods are almost the same. However, when these methods are used to calculate the ultimate strength of the ship, the calculation time required by each method is different, and the time required byMethod 3 is much

less than the others. The research of the calculation code shows that calculating the stress of the units requires the most time because the number of the units is large and they need to be calculated many times to search for the location of NA. Therefore, the calculation efficiency depends on number of calculations of unit stress. Then the average time required by the 3 methods to calculate the unit stress is shown in Table 12.

Table 12. Number of calcuations required to obtain the unit stress.

	Method 1	Method 2	Method 3
Average number of calculations	703	32041	15

It can be seen that the number of calculations required by Method 3 is much less than other two methods, which is 2.13% of Method 1 and 0.05% of Method 2, thus the calculation efficiency of the method proposed in this paper is much higher than the other methods.

5. Conclusions

In this paper, an improved force vector equilibrium criterion is proposed for the calculation of the location of NA of asymmetric section. Based on the analytic derivation of the relationship between the location of NA and the criteria, a Smith method based on the linear equation is proposed. Validation of the method carried out for the ultimate strength of a VLCC shows that the method is accurate and very efficient. Based on the analysis of the results, some conclusions are drawn:

(1) When the CNA of the cross-section translates or rotates near the location of NA, the results of the force equilibrium criterion and the improved force vector equilibrium criterion are approximately linear with the translation or rotation of the CNA. These linear relationships can be derived from the location of NA, and are found to be independent for the height and the angle throughout the entire calculation process. However, the relationships become nonlinear when the CNA is located far away from NA.

(2) A linear equation can be established to derive the location of NA according to this linear relationship, and the equation is obtained by the results of the criterion for different locations of the CNA. The linear equation of the force equilibrium criterion is only used to obtain the height of NA, and the improved force equilibrium criterion is only used to obtain the angle of NA.

(3) By analyzing the FEC and the IFVEC, the tolerances have been optimized to improve the accuracy of the results of the location of NA. The proposed method is validated by calculating the ultimate strength of a VLCC, and it is shown that it is accurate and much more efficient than the methods exisiting in the literature.

Acknowledgements

This study is supported by the “National Key Technologies Research & Development Program” (2022YFB3306200) and the “National Natural Science Foundation of China” (Grant No. 52171305).

References

Ahn H.J., Baek D.P., Lee T.K. 2011. A Study on Residual Strength Assessment of Damaged Oil Tanker by Smith Method. Journal of Korean navigation and port research. 35(10), 823–827.

Campanile A., Piscopo V., Scamardella A. 2014. Statistical properties of bulk carrier longitudinal strength. Mar Struct. 39, 438–462.

Campanile A., Piscopo V., Scamardella A. 2015. Statistical properties of bulk carrier residual strength. Ocean Engineering. 106, 47–67.
Chan H.S., Atlar M., Incecik A. 2003. Global Wave Loads on Intact and Damaged Ro-Ro Ships in Regular Oblique Waves. Marine Structures. 16, 323–344.
Chan H.S., Incecik A., Atlar M. 2001. Structural Integrity of a Damaged Ro-Ro Vessel. In Proceedings of the Second International Conference on Collision and Grounding of Ships. Technical University of Denmark, Lyngby, Denmark, 253–258.
Choung J., Nam J.M., Ha T.B. 2012. Assessment of residual ultimate strength of an asymmetrically damaged tanker considering rotational and translational shifts of neutral axis surface. Marine Structures. 25(1), 71–84.
Choung J., Nam J.M., Tayyar G.T. 2014. Residual ultimate strength of a very large crude carrier considering probabilistic damage extents. International Journal of Naval Architecture and Ocean Engineering. 6(1), 14–26.
EMSA, 2019. Annual overview of marine casualties and incidents 2019. European Maritime Safety Agency (EMSA), Lisboa, Portugal.
Faisal M., Noh S.H., Kawsar M.R.U., Youssef S.A.M., Seo J.K., Ha Y.C., Paik J.K. 2017. Rapid hull collapse strength calculations of double hull oil tankers after collisions. Ships and Offshore Structures. 12(5), 624–639.
Fang C., Das P.K. 2005. Survivability and reliability of damaged ships after collision and grounding. Ocean Engineering. 32(3–4), 293–307.
Fujikubo M., Alie M.Z.M., Takemura, K., Iijima, K., Oka, S., 2012. Residual Hull Girder Strength of Asymmetrically Damaged Ships. Journal of the Japan Society of Naval Architects and Ocean Engineers. 16(0), 131–140.
Hu K., Yang P., Xia T., Peng Z. 2018. Residual ultimate strength of large opening box girder with crack damage under torsion and bending loads. Ocean Engineering. 162, 274–289.
Hussein A. W., Guedes Soares C. 2009. Reliability and residual strength of double hull tankers designed according to the new IACS common structural rules. Ocean Engineering. 36(17–18), 1446–1459.
IACS, 2014. Harmonized Common Structural Rules for Oil Tankers and Bulk Carriers. International Association of Classification Societies, London, UK.
Kuznecovs A., Ringsberg J.W., Johnson E., Yamada Y. 2020. Ultimate limit state analysis of a double-hull tanker subjected to biaxial bending in intact and collision-damaged conditions. Ocean Engineering. 209, 1–15.
Li C.F., Fu P., Ren H.L., Xu W.J., Guedes Soares C. 2017. Ultimate Bearing Capacity Assessment of Hull Girder with Asymmetric Cross-Section. In Proceedings of the 36th International Conference on Offshore Mechanics and Arctic Engineering (OMAE), Trondheim, Norway. 140(6), 1–9.
Li C.F., Gao C., Zhou X.Q., Dong S., Fu P., Xu D.H. 2018. A PSO-Based Method for Tracing the Motion of Neutral Axis Surface of Asymmetric Hull Cross-Sections and Its Application. In Proceedings of the 37th International Conference on Offshore Mechanics and Arctic Engineering, Madrid, Spain, 3, 1–12.
Liu Z., Amdahl J. 2012. Numerical and simplified analytical methods for analysis of the residual strength of ship double bottom. Ocean Engineering. 52, 22–34.
LR, 2020. Rules and regulations for the classification of naval ships. Lloyd's Register (LR), London, UK.
Luís R.M., Hussein A.W. Guedes Soares C. 2007. On the effect of damage to the ultimate longitudinal strength of double hull tankers. 10th International Symposium on Practical Design of Ships and Other Floating Structures. 1(1995), 354–362.

Paik J.K., Amlashi H., Boon B., Branner K., Caridis P., Das P., Fujikubo M., Huang C.H., Josefson L., Kaeding P. 2012. Committee III.1 Ultimate Strength. In Proceedings of the 18th International Ship and Offshore Structures Congress (ISSC), Rostock, Germany.

Parunov J., Rudan S., Gledić I., Bužančić Primorac B. 2018. Finite element study of residual ultimate strength of a double hull oil tanker with simplified collision damage and subjected to bi-axial bending. Ships and Offshore Structures. 13(1), 25–36.

Shi G.J., Gao D.W. 2021. Model experiment of large superstructures' influence on hull girder ultimate strength for cruise ships. Ocean Engineering. 222, 1–10.

Smith C.S. 1977. Influence of Local Compression Failure Compression Failure on Ultimate Longitudinal Strength of Ship Hull. In Proceeding of the International Symposium on Practical Design in Shipbuilding. Tokyo, Japan, 73–79.

Tekgoz M., Garbatov Y., Guedes Soares C. 2018. Strength assessment of an intact and damaged container ship subjected to asymmetrical bending loadings. Marine Structures. 58, 172–198.

Yao T., Asrup O.C., Caridis P., Chen Y.N., Cho S.R., Dow R.S., Niho O., Rigo P. 2000. Special Task Committee VI.2: Ultimate Hull Girder Strength. In Proceedings of the 14th International Ship and Offshore Structures Congress (ISSC), Nagasaki, Japan.